# ECG reconstruction based on the injection of a multi-frequency signal in capacitive measurement systems

A. Serteyn, R. Vullings, M. Meftah and J.W.M. Bergmans

***Abstract*— Many healthcare and lifestyle applications could benefit from capacitive measurement systems for unobtrusive ECG monitoring. However, a key technical challenge remains: the susceptibility of such systems to motion artifacts and common-mode interferences. With this in mind, we developed a novel method to reduce various types of artifacts present in capacitive ECG measurement systems. The objective is to perform ECG reconstruction and channel balancing in an automated and continuous manner. The proposed method consists of *a*) modeling the measurement system; *b*) specifically parameterizing the reconstruction equation; and *c*) adaptively estimating the parameters. A multi-frequency injection signal serves to estimate and track the variations of the different parameters of the reconstruction equation. A preliminary investigation on the validity of the method has been performed in both simulation and lab environment: the method shows benefits in terms of common-mode interference and motion artifact reduction, resulting in improved R-peak detection.**

## I. Introduction

Capacitive electrodes are a promising and more comfortable alternative to the conventional adhesive electrodes for healthcare and lifestyle applications; they allow the recording of biopotentials, such as the electrocardiogram (ECG), through several layers of insulating materials. Capacitive electrodes have therefore been considered as a promising technology to facilitate clinical procedures (no skin-preparation time) or to be embedded in everyday objects, such as beds or car seats, for long-term monitoring. However, despite their recent commercialization [1], capacitive electrodes are still highly sensitive to motion artifacts.

State-of-the-art capacitive measurement systems feature a single-frequency injection signal to detect loose electrodes [2] or continuously measure the impedance of the body-electrode interface [3] as it is commonly done in conventional ECG systems [4], [5]. The continuous measurement of impedance, when combined with adaptive filters, has been shown to help in reducing motion artifact in conventional ECG systems [6] as well as in capacitive systems [7]. In this study, we go one step further and propose to use a multi-frequency injection signal in an effort to automatically reconstruct an ECG signal free from artifacts.

To perform ECG signal reconstruction in capacitive systems, a model has been previously proposed and tested in a lab bench environment in [8]. The electrode coupling was assumed to be purely capacitive and all parameters of the reconstruction equation were known or manually tuned to obtain the best reconstruction results. Here, we extend the model to include a resistive component in parallel with the coupling capacitor, and, consequently, provide a more general reconstruction equation than in [8]. Then, a multi-frequency injection signal is exploited to estimate the different parameters of the model automatically. The proposed method is thus entirely software-based, fully automated and can be seen as a reverse filtering of the measured ECG signal. The method is expected to reduce additive artifacts and signal distortions due to variation of the coupling impedance. When used in a bipolar measurement setup (two measuring capacitive electrodes), the proposed method could also reduce differential-mode artifacts due to common-mode interferences. Some preliminary results in simulation environment and in a lab bench experiment are presented.

A. Serteyn, R. Vullings and J.W.M. Bergmans are with the Faculty of Electrical Engineering, University of Technology Eindhoven, 5612 AZ, Eindhoven, The Netherlands a.a.m.serteyn@tue.nl

M. Meftah is with the Patient Care Solutions group, Philips Research Eindhoven, The Netherlands

## II. Method

### A. Model of the capacitive system

An equivalent circuit for the capacitive measurement system is represented in Fig. 1. It combines the models proposed in [8], [9] and [7]. The parasitic voltage $V_d$ originates

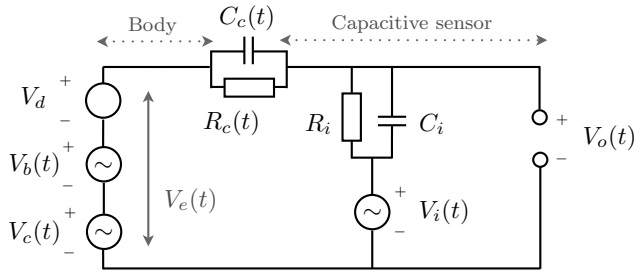


Fig. 1. Equivalent circuit of the capacitive measurement system, adapted from [8], [9] and [7].

partly from the accumulation of charges on the body and on the electrode due to the triboelectric effect [9]. We assume here that $V_d$ is constant or slowly drifting. The time variations of the coupling capacitance $C_c(t)$ and resistance $R_c(t)$ in combination with $V_d$ cause a motion artifact in $V_o(t)$. A multi-frequency signal $V_i(t)$ is injected from the electrode side to track the impedance variations at the body-electrode interface ($C_c$ and $R_c$ variations). The voltage $V_c(t)$ represents the common-mode voltage, i.e. it is identical for each capacitive electrode in an array. The common-mode voltage can be due to the power lines (50-60 Hz) but also to the motion of a charged body in the environment of the

978-1-4244-7929-0/14/$26.00 ©2014 IEEE

capacitive electrode [10], [9]. The input resistance $R_i$ and input capacitance $C_i$ of the electrode amplifier are constant over time but different for each electrode. The voltage $V_b(t)$ is the biopotential of interest, here an ECG. For clarity, the sum of the voltages $V_b(t)$, $V_c(t)$ and $V_d$ is defined as $V_e(t)$. Typical values of the model parameters are listed in Table I.

TABLE I
TYPICAL VALUES OF THE MODEL PARAMETERS

| Parameter | Symbol | Value | Frequency band |
|---|---|---|---|
| Bias resistance | $R_i$ | 50 GΩ | 0 |
| Input capacitance | $C_i$ | 2.8 pF | 0 |
| Coupling resistance | $R_c$ | [0.1 $+\infty$] GΩ | [0 10] Hz |
| Coupling capacitance | $C_c$ | [0.5 8] pF | [0 10] Hz |
| Parasitic static voltage | $V_d$ | [0 1] V | 0 |
| Injection signal | $V_i$ | 5 $\mathrm{mV_{pp}}$ | [1 300] Hz |
| Biopotential | $V_b$ | 1.3 $\mathrm{mV_{pp}}$ | [0.5 40] Hz |

By analysing the equivalent circuit of Fig. 1, we obtain the time domain behavior of the capacitive measurement system:

$$\begin{aligned} &C_c\frac{\mathrm{d}(V_e-V_i)}{\mathrm{d}t}+\Big(\frac{1}{R_c}+\frac{\mathrm{d}C_c}{\mathrm{d}t}\Big)(V_e-V_i)\\ &=(C_c+C_i)\frac{\mathrm{d}(V_o-V_i)}{\mathrm{d}t}+\Big(\frac{1}{R_i}+\frac{1}{R_c}+\frac{\mathrm{d}C_c}{\mathrm{d}t}\Big)(V_o-V_i), \end{aligned} \tag{1}$$

where $C_c$, $R_c$, $V_o$, $V_i$, and $V_e = V_b + V_d + V_c$ are time-varying.

Solving (1) for $V_e - V_i$ using standard techniques for differential equations with time-varying coefficients [11] yields the reconstruction equation for $V_e(t)$:

$$\begin{aligned} V_e-V_i=\frac{\mathrm{e}^{-\int_{t_0}^{t}\frac{1}{C_cR_c}\mathrm{d}s}}{C_c}\Bigg(\int_{t_0}^{t}\mathrm{e}^{\int_{t_0}^{u}\frac{1}{C_cR_c}\mathrm{d}s}\Big((C_i+C_c)\frac{\mathrm{d}(V_o-V_i)}{\mathrm{d}u}\\ +\big(\frac{1}{R_c}+\frac{1}{R_i}+\frac{\mathrm{d}C_c}{\mathrm{d}u}\big)(V_o-V_i)\Big)\mathrm{d}u+\alpha\Bigg), \end{aligned} \tag{2}$$

where

$$\alpha = C_c(t_0)V_e(t_0).$$

When there is no common-mode interference, $V_c(t) = 0$ and $V_e(t)$ is nothing else than $V_b(t)$ plus an offset $V_d$ which can be easily removed by high-pass filtering. In the presence of a common-mode voltage $V_c(t)$, the reconstructed signal from a second electrode $V_{e2}(t)$ is subtracted from $V_e(t)$ to provide the bipolar ECG signal $V_b(t) - V_{b2}(t)$.

### B. Parametrization of the reconstruction equation

The reconstruction equation (2) can be parameterized with three parameters, $X(t)$, $Y(t)$ and $K$ that are function of the 4 unknown system components $R_c(t), C_c(t), R_i$, and $C_i$:

$$X(t)=\frac{C_c(t)}{C_i},\ Y(t)=\frac{1}{C_iR_c(t)},\ \text{and}\ K=\frac{1}{C_iR_i}$$

Substituting these parameters in the equation for $V_e - V_i$ results in

$$\begin{aligned} V_e-V_i=\frac{\mathrm{e}^{-\int_{t_0}^{t}\frac{Y}{X}\mathrm{d}s}}{X}\Bigg(\int_{t_0}^{t}\mathrm{e}^{\int_{t_0}^{u}\frac{Y}{X}\mathrm{d}s}\Big((1+X)\frac{\mathrm{d}(V_o-V_i)}{\mathrm{d}u}\\ +\big(Y+K+\frac{\mathrm{d}X}{\mathrm{d}u}\big)(V_o-V_i)\Big)\mathrm{d}u+\alpha\Bigg). \end{aligned} \tag{3}$$

With this equation and with known parameters $V_i(t)$, $X(t)$, $Y(t)$, and $K$, a complete reconstruction of the signal $V_e(t)$ is possible. In practice, the parameters $X(t), Y(t)$ and $K$ are not known and must therefore be estimated before any reconstruction is possible. Note that in the particular case where $R_c \to +\infty$, $Y(t)$ approaches zero and the reconstruction equation reduces to

$$V_e = V_o + \frac{1}{X}(V_o - V_i) + \frac{K}{X}\int_{t_0}^{t}(V_o - V_i)\mathrm{d}u + \frac{\alpha}{X}, \tag{4}$$

which agrees with the work of Heuer et al. [8].

### C. Parameter estimation

A known injection signal $V_i(t)$ composed of sinusoids at several frequencies is applied from the capacitive electrode side, propagates through the measurement system and is measured at the output $V_o(t)$. The transformation of this signal during the measurement process is directly related to the values and variations of the different model parameters $X(t)$, $Y(t)$, and $K$ and can therefore be used for their estimation.

*1) Parameter $X(t)$:* The parameter $X(t)$ depends only on the coupling and input capacitances. At sufficiently high frequencies, the capacitances suffice to describe the system behavior and the resistances in (1) can be assumed infinite. In this way, the transfer of $V_i(t)$ to the output $V_o(t)$ reduces to a real-valued gain

$$g(t)=\frac{V_o(t)}{V_i(t)}\approx\frac{C_i}{C_i+C_c(t)},$$

which represents the amplitude modulation of $V_i(t)$ at high frequencies. We can obtain $g(t)$ by demodulating $V_o(t)$ at a given high frequency. An estimate $\tilde{X}(t)$ for the parameter $X(t)$ is then directly computed as

$$\tilde{X}(t)=\frac{1-g(t)}{g(t)}\approx\frac{C_c(t)}{C_i}.$$

*2) Parameters $K$ and $Y(t)$:* The parameter $K$ depends on intrinsic components of the electrode and is therefore slightly different for each electrode but relatively constant over time. The parameter $Y(t)$ is inversely proportional to the coupling resistance $R_c(t)$. For $R_c(t)$ in the order of several TΩ, $Y(t)$ approaches zero and does not influence the measurement process; the variations of $X(t)$, i.e. of $C_c(t)$, are the dominant cause for the artifact. For small values of $R_c(t)$ (a few GΩ in capacitive systems), $Y(t)$ dominates $X(t)$ and is the principal cause for the artifact measured in $V_o(t)$. Parameters $K$ and $Y$ are estimated together. Starting from $V_o - V_i$, $\tilde{X}$, and some initial values for

$K$ and $Y$, the signal reconstruction is performed using the right-hand side of (3) with $\alpha = 0$. The obtained reconstructed signal is designated $V_r(t)$. The objective is to perform a perfect reconstruction, i.e. to estimate $K$ and $Y$ such that $V_r = V_e - V_i$ or $V_r + V_i = V_e$. The parameter estimation should therefore guaranty that $V_r + V_i$ does not contain any component of $V_i$ anymore. In that regard, we chose to estimate $K$ and $Y$ by minimizing the root mean square (RMS) amplitude of $V_r + V_i$ on each processing window. This adaptive method is schematically represented in Fig. 2. The

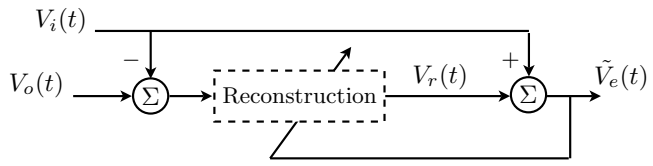


Fig. 2. Adaptive scheme for the estimation of parameters $K$ and $Y$. The reconstruction is performed as in (3).

parameter estimation with this chosen optimization criteria will perform best for $V_e = 0$, which is not always achievable in practice. More particularly, the biopotential $V_b(t)$ and the common mode $V_c(t)$ directly influence the RMS amplitude of $V_r(t)$ and therefore hamper the parameter estimation. The influence of these signals can be reduced by performing the reconstruction on long windows, however, this will hamper tracking of the fast-varying parameter $Y(t)$. A compromise is made by choosing sliding reconstruction windows of one second and by setting a lower limit for the difference of the RMS amplitude of $V_o(t)$ and $V_r(t)$. This avoids tracking the amplitude variations of $V_b$ and $V_c$.

Note that, with these estimation procedures, there is a limit on how fast $Y(t)$ can be tracked while there is none for $X(t)$. Note also that, in static conditions, e.g. before starting the measurement process, the parameter estimation corresponds to a common channel balancing process, which is a useful method to avoid the differential-mode artifacts that occur when a common-mode interference is recorded by two slightly different electrodes.

## III. Results and discussion

### A. Static conditions

First, the validity of the method is illustrated in simulation in static conditions. In the absence of motion and in a bipolar measurement setup, the reconstruction method acts as software-based channel balancing. By reconstructing the ECG signals of each electrode individually, we compensate for any mismatch between the two recording electrodes. This mismatch depends not only on the electrode's internal design (in terms of $R_i$ and $C_i$) but also, and mostly, on the coupling interface (in terms of $R_c$ and $C_c$). When the two channels are balanced, i.e. when the signal of each channel has been reconstructed, common-mode interferences can be reduced by taking the difference between the two signals.

Capacitive electrodes, with their high input-impedance, are particularly sensitive to environmental common-mode interferences. The motion of a person in the environment of the capacitive measurement system for example can create common-mode interferences. This scenario has been simulated in MATLAB and is illustrated in Fig. 3. The two

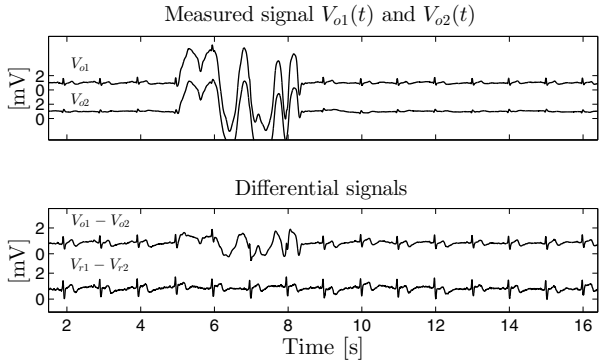


Fig. 3. Example of channel balancing on simulation data. A differential-mode artifact is present in $V_{o1} - V_{o2}$ (upper trace of the second panel) but not in $V_{r1} - V_{r2}$ (lower trace).

signal $V_{o1}(t)$ and $V_{o2}(t)$ in the upper graph represent the signal measured at the output of two different electrodes. A common mode signal $V_c(t)$ is applied to each electrode starting at 5 s. These signals were generated from (1) implemented in Simulink (The Mathworks) with the parameter values given in Table II. The frequencies of the injected

TABLE II
Parameter value used for the simulation of two unbalanced recording electrodes

| Electrode | $R_c$ | $C_c$ | $R_i$ | $C_i$ |
|---|---|---|---|---|
| 1 | 4 GΩ | 4 pF | 50 GΩ | 2.8 pF |
| 2 | 10 GΩ | 2 pF | 48 GΩ | 3 pF |

sinusoids were 2, 4, 8 and 64 Hz, each of which having an amplitude of 5 mV. The highest frequency, 64 Hz, is used for the estimation of the parameter $X(t)$ as described in subsection II-C.1. The lower frequencies are required for the estimation of the parameters dependent on the resistances of the circuit, i.e. $Y(t)$ and $K$. Another combination of low and high frequencies could be chosen with little impact on the results. The window size for the parameter estimation and ECG signal reconstruction was 1 second and the reduction in RMS amplitude during the parameter estimation loop was constrained to a minimum of 34 mV.

The second panel of Fig. 3 illustrates that calculating the difference between the two electrode outputs is not sufficient to remove the common-mode artifact; a differential-mode artifact remains in $V_{o1} - V_{o2}$. However, when first reconstructing (reverse filtering) the signals $V_{o1}(t)$ and $V_{o2}(t)$ using the proposed method before calculating their difference ($V_{r1} - V_{r2}$), the common mode artifact is fully rejected. Note that the 1-s window size allows the channel balancing process to adapt, with one second delay, to a change of the measurement conditions, e.g. a change of body position for capacitive electrodes embedded in a sleeping mattress.

### B. Dynamic conditions

The proposed method was also applied on lab data as an illustration of the potential use for artifact reduction. The lab data were originally recorded for another purpose than illustrating the performance of the present method, therefore, only two sinusoids at 70 and 90 Hz were injected. The lab setup consisted of a metal plate on which an artificial ECG was applied. The capacitive electrode was coupled to the metal plate via an air gap. The metal plate was moved up and down in a sweep-like manner to create capacitance variations at the plate-electrode interface. The measured signal $V_o(t)$, represented in the upper graph of Fig. 4, was sampled at 8 kHz. Because of the air gap, the coupling interface can be considered purely capacitive and (4) is used for the ECG reconstruction. The parameter $X(t)$ was estimated by demodulating $V_o(t)$ at 90 Hz and the constant and unknown parameter $\alpha$ was estimated on a 2-s window by minimizing the RMS amplitude of $V_r + V_i$. The output of the automated reconstruction is shown in the bottom graph of Fig. 4.

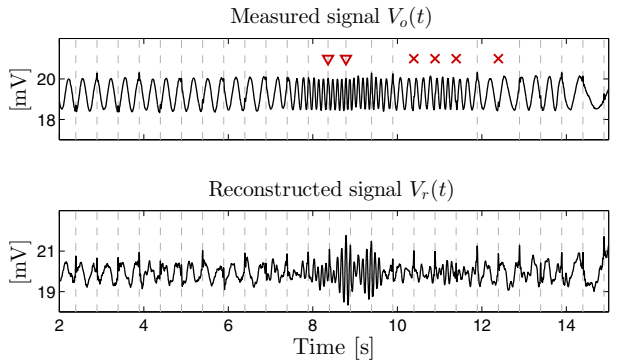


Fig. 4. Example of signal reconstruction on lab data. Although the shape of the signal is not fully recovered, all heart beats in $V_r(t)$ are correctly detected as shown by the vertical dashed lines. The symbols $\nabla$ and $\times$ indicate, respectively, shifted peaks and missed peaks.

We observe that the reconstructed signal $V_r(t)$ has a much larger signal to artifact ratio than the measured signal $V_o(t)$. Also, the artifact is not only reduced as in [7] but the R-peaks are enhanced (distortion compensation). And although this is not sufficient to make the full ECG shape clearly visible, it significantly improves the performance of a state-of-the art heart-beat detection algorithm [12]. Two beats were detected as shifted in $V_o(t)$ (see $\nabla$) and 4 were missed (see $\times$), while all heart beats in $V_r(t)$ were correctly detected as illustrated by the vertical dotted lines in Fig. 4.

## IV. Conclusion and Future Work

The proposed method is designed to compensate, on the one hand, for distortions of the measured ECG due to dynamic filtering effects and, on the other hand, for additive artifacts created by the combination of movement at the body-electrode interface in the presence of a static charge $V_d$. Moreover, when two electrodes are available, the common mode artifact can be fully suppressed in simulation because of the channel balancing. The method is also entirely automated and works in software in an online manner, which makes it easy to use in combination with any capacitive measurement system featuring injection signals. Simulation results suggest that the method is very well suited for the automatic removal of differential-mode artifacts in a pair or array of capacitive electrodes. It also shows a high potential for improved peak detection on lab data. The method could thus be used as it is, but also as preprocessing step for array processing techniques aiming at removing, for example, the triboelectric artifact.

Although the method can track fast variations of $X(t)$, it is not yet able to track fast variations of the parameter $Y(t)$. Indeed, the $Y(t)$ estimation (Section II-C.2) is performed on relatively long windows to avoid tracking $V_b(t)$ and $V_c(t)$. A refinement of the minimization criteria for the estimation of $Y(t)$, for example by combining a minimization of the RMS amplitude of $V_r + V_i$ with a minimization of the correlation between $V_r + V_i$ and $V_i$, might be beneficial to address this issue and achieve high quality reconstruction performances. Extended lab experiments with a different set of injection frequencies and layers of different materials at the coupling interface (instead of an air gap) are needed to further validate the proposed method.

## References


[1] (2014, April) http://nl.mouser.com/new/Plessey-Semiconductors/plessey-ps25xxx-sensors/.

[2] T. Wartzek, H. Weber, M. Walter, B. Eilebrecht, and S. Leonhardt, "Automatic electrode selection in unobtrusive capacitive ECG measurements," in *IEEE CBMS*, 2012, pp. 1–4.

[3] B. Eilebrecht, J. Willkomm, A. Pohl, T. Wartzek, and S. Leonhardt, "Impedance measurement system for determination of capacitive electrode coupling," *IEEE Trans. Biomed. Eng.*, vol. PP, no. 99, pp. 1–1, 2013.

[4] D. Buxi, *et al.*, "Correlation between electrode-tissue impedance and motion artifact in biopotential recordings," *Sensors Journal, IEEE*, vol. 12, no. 12, pp. 3373 –3383, 2012.

[5] T. Degen and H. Jackel, "Continuous monitoring of electrode–skin impedance mismatch during bioelectric recordings," *IEEE Trans. Biomed. Eng.*, vol. 55, no. 6, pp. 1711–1715, June 2008.

[6] P. Hamilton, M. Curley, R. Aimi, and C. Sae-Hau, "Comparison of methods for adaptive removal of motion artifact," in *Computers in Cardiology 2000*, 2000, pp. 383–386.

[7] A. Serteyn, R. Vullings, M. Meftah, and J. W. M. Bergmans, "Using an injection signal to reduce motion artifacts in capacitive ECG measurements," in *EMBS, 35th Annu. Int. Conf. IEEE*, 2013, pp. 4795–4798.

[8] S. Heuer, D. Martinez, S. Fuhrhop, and J. Ottenbacher, "Motion artefact correction for capacitive ECG measurement," in *Biomedical Circuits and Systems Conference. IEEE*, 2009, pp. 113 –116.

[9] T. Wartzek, T. Lammersen, B. Eilebrecht, M. Walter, and S. Leonhardt, "Triboelectricity in capacitive biopotential measurements," *IEEE Trans. Biomed. Eng.*, vol. PP, no. 99, p. 1, 2010.

[10] D. H. Gordon, "Triboelectric interference in the ecg," *IEEE Trans. Biomed. Eng.*, vol. BME-22, no. 3, pp. 252–255, May 1975.

[11] T. Apostol, *Calculus, vol. 1: One-variable calculus with an introduction to linear algebra*. Wiley New York, 1967.

[12] M. J. Rooijakkers, C. Rabotti, S. G. Oei, and M. Mischi, "Low-complexity R-peak detection for ambulatory fetal monitoring," *Physiological Measurement*, vol. 33, no. 7, pp. 1135 – 1150, 2012.